INSTITUTE OF PHYSICS PUBLISHING JOURNAL OF PHYSICS B: ATOMIC, MOLECULAR AND OPTICAL PHYSICS

J. Phys. B: At. Mol. Opt. Phys. **35** (2002) 4657–4667 PII: S0953-4075(02)38140-9

Total and elastic electron scattering cross sections from Xe at intermediate and high energies

G García[1], J L de Pablos[2], F Blanco[3] and A Williart[4]

[1] Instituto de Matemáticas y Física Fundamental, CSIC, Serrano 123, 28006 Madrid, Spain
[2] Departamento de Fusión y Partículas Elementales, CIEMAT, Avenida Complutense 22, 28040 Madrid, Spain
[3] Departamento de Física Atómica Molecular y Nuclear, Universidad Complutense de Madrid, 28040 Madrid, Spain
[4] Departamento de Física de los Materiales, UNED, Senda del Rey 9, 28040 Madrid, Spain

Received 13 June 2002, in final form 30 September 2002
Published 4 November 2002
Online at stacks.iop.org/JPhysB/35/4657

Abstract

Experimental total electron scattering cross sections from Xe in the energy range 300–5000 eV have been obtained with experimental errors of about 3%. The method was based on the measurement of the attenuation of a linear electron beam through a Xe gas cell in combination with an electron spectroscopy technique to analyse the energy of the transmitted electrons. Differential and integral elastic cross sections have been calculated using a scattering potential method which includes relativistic effects. The consistency of our theoretical and experimental results is also discussed in the paper. Finally, analytical formulae depending on two parameters, namely the number of target electrons and the atomic polarizability, are given to reproduce the experimental data for Ne, Ar, Kr and Xe in the energy range 500–10 000 eV.

1. Introduction

Energy deposition models to study radiation interaction with matter and radiation damage require scattering cross section data for secondary electrons over a wide energy range. In principle, data for all of the possible processes are needed for energies ranging from the high energy of the primary particles down to the low energies of those electrons degraded by successive collisions. In this process, total cross sections play an important role in defining the mean free path for simulations and providing a way to put on an absolute scale to relative cross section data. Noble gases can be considered as reference atomic targets and are commonly used to check the validity of theoretical approximations by comparison with accurate experimental data. For this reason considerable effort has been devoted to obtaining reliable sets of total electron scattering cross section data for these targets and the main results can be found in several compilations (see [1, 2]). However, at high energy important discrepancies exist between the results obtained in linear transmission-beam experiments [3] and those derived

from a modified Ramsauer apparatus [4]. This unsatisfactory situation motivated further experimental and theoretical verifications [5, 6]. As pointed out by Zecca *et al* [7] in a recent comment, this discrepancy is strongly dependent on the size of the target—being practically negligible for neon but of the order of 40% for Kr at 4000 eV. In the particular case of Xe, for energies above 700 eV, no total cross section measurements have been performed in a linear experiment. Reference [7] concluded that the origin of this target dependence was not still clear and that small-angle scattering experiments were needed to clarify it. These considerations motivated this work.

In this study, accurate total cross sections, within 3%, for electron scattering by Xe have been measured in the energy range 300–5000 eV by means of a transmission-beam technique. Differential and integral elastic cross sections have been calculated up to 10 000 eV by a scattering potential method including relativistic corrections. These experimental results have been added to those of Ne, Ar and Kr that are already available in the literature, in order to obtain empirical formulae reproducing accurately the experimental data. As a consequence, the origin of the discrepancy mentioned above has been clarified.

2. Experiment

The experimental apparatus used in this study was based on a previously described one [3] and will be only briefly reviewed in this paper. The primary electron beam, produced by an emitting filament, was collimated into a 1 mm diameter and deflected by a combination of electrostatic plates with a transverse magnetic field. Typical operating currents for the attenuation measurements were between 10^{-13} and 10^{-14} A. The energy spread under these conditions was around 500 meV. The collision chamber was defined by two apertures, each of 1 mm diameter separated by a length of 100 mm. The gas pressure in the chamber was measured with an absolute capacitance manometer (MKS Baratron 127 A). The transmitted electrons were energy analysed by an electrostatic hemispherical spectrometer combined with a retarding field. Under these conditions a constant energy resolution of about 0.8 eV (FWHM) was obtained over the whole energy range reported here. The acceptance angle of the analyser was of the order of 10^{-5} sr. Electrons were detected at the exit of the energy analyser by a two-stage microchannel plate operating in pulse counting mode. A typical energy loss spectrum of electrons scattered into the detector angle is shown in figure 1. In this figure, the asymmetry of the elastic peak is due to the time constant of the counting system. The ultimate pressure in the region of the energy analyser and electron detector was of the order of 10^{-7} Torr.

3. Elastic cross section calculations

The scattering potential method used in this work to calculate both differential ($\mathrm{d}\sigma_{el}/\mathrm{d}\Omega$) and integral elastic ($\sigma_{el}$) cross sections has been described in [6]. These parameters have been obtained from a partial wave expansion, which can be written as a function of the incident electron momenta (k), the Legendre polynomial $P_l(\cos\theta)$ and the phase shifts (δ_l) as

$$\frac{\mathrm{d}\sigma_{el}}{\mathrm{d}\Omega} = \frac{1}{4k^2}\left|\sum_{l=0}^{l_{max}}(2l+1)(\mathrm{e}^{2\mathrm{i}\delta_l}-1)P_l(\cos\theta)\right|^2 \tag{1}$$

and

$$\sigma_{el}(E) = \frac{4\pi}{k^2}\sum_{l=0}^{l_{max}}(2l+1)\sin^2\delta_l, \tag{2}$$

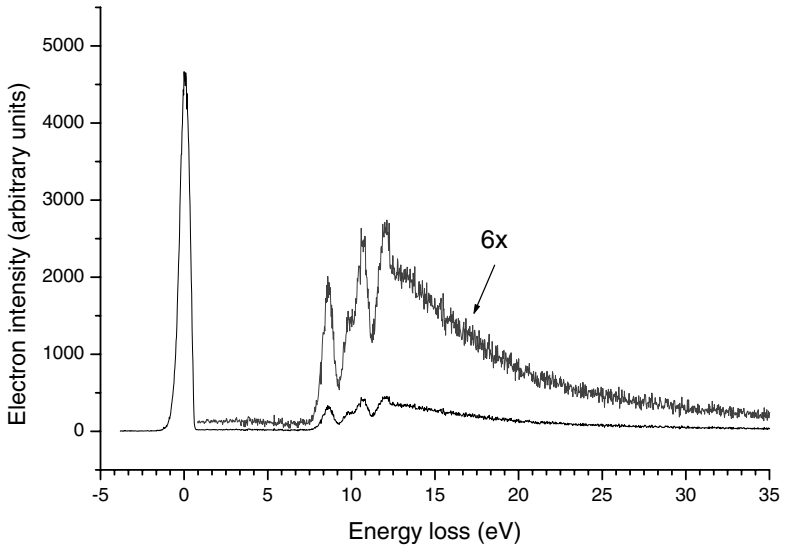

Figure 1. Energy loss spectrum for 2000 eV incident electrons and 20 mTorr of Xe in the gas cell.

respectively. The lth partial wave phase shift δ_l has been obtained by integrating the scattering equation for the corresponding radial wavefunction using an adaptive-step-size fourth-order Runge–Kutta algorithm [8] based on a variable-phase technique [9]. Accordingly, the following first-order nonlinear equation, in terms of the $j_l(t)$ and $n_l(t)$ Riccati–Bessel functions, has been solved:

$$\delta_l'(r) = -\frac{2}{k}V(r)[\cos\delta_l(r)\,\hat{j}_l(kr) - \sin\delta_l(r)\hat{n}_l(kr)]^2 \tag{3}$$

with $\delta_l(0) = 0$, $\delta_l'(0) = 0$. The potential $V(r)$ includes electrostatic interaction with the atomic charge density, polarization of the target, exchange effects and relativistic corrections. The relativistic effects have been considered both in the Hartree–Fock wavefunction calculations to determine the atomic charge density and in solving the phase shift equations. Since the relativistic corrections behave near the origin as $1/r^2$, the above initial conditions for the phase shift had to be changed for $l = 0$ to

$$\delta_0(0) = 0, \qquad \delta_0'(0) \approx -\frac{k}{9}(3 - 2\alpha^2 Z^2), \tag{4}$$

where α and Z are the fine-structure constant and the number of electrons of the target, respectively.

4. Results and discussion

4.1. Total scattering cross sections

Our electron scattering total cross sections from xenon in the energy range 300–5000 eV are listed in table 1 together with other experimental data available in the literature [10–13]. As may be seen, for energies between 300 and 750 eV there is a general agreement to within 12%. In particular, our results show an excellent agreement within 3% with those of Wagenaar and de Heer [10] and Nickel *et al* [12]. However, above this energy range the only previous measurements of Zecca *et al* [4] tend to be lower than ours, reaching discrepancies of the

Table 1. Experimental total cross sections for electron scattering by xenon in the energy range 100–5000 eV in atomic units (a_0^2).

Energy (eV)	This work (±3%)	Wagenaar and de Heer [10]	Dababneh *et al* [11]	Nickel *et al* [12]	Zecca *et al* [4]	Szmytkowski *et al* [13]
100		43.51	38.69	42.50	43.7	41.78
125		41.44	37.21	39.75		
150		39.40	34.9	37.96		
200		36.02	32.5	35.43		33.96
250		33.27	30.0	32.88		
300	31.6	30.95	28.1	30.53		
350	29.6	28.93	26.1			
400	28.0	27.32	24.7		25.87	
500	24.9	24.53	21.9			
600	22.9	22.38	19.2			
700	20.9	20.56	18.5			
800	19.3					
900	18.1				16.13	
1000	17.1				14.90	
1250	14.9					
1500	13.5					
1750	12.4					
2000	11.5				9.58	
2500	10.2				8.25	
3000	9.19				7.42	
3500	8.42				6.73	
4000	7.80				6.11	
4500	7.28					
5000	6.89					

order of 30% at 4000 eV. Similar discrepancies between the results of the Madrid [3, 6] and Trento [4, 5] laboratories have been found for other targets, these discrepancies being the subject of further investigations [14–16] in the last few years. Although the mean cause seems to be the poorer angular and energy resolution of the Trento apparatus, Zecca *et al* [7] pointed out that it is not still clear why the magnitude of these discrepancies depends on the size of the target, being practically negligible in the case of Ne. In order to understand this different behaviour, figure 2 shows a plot of the energy spectra of transmitted electrons through 10 mTorr of Ne, Ar, Kr and Xe, respectively, at 2525 eV incident energy. At this energy, the energy resolution of our system was better than 1 eV (FWHM), hence the inelastic component is completely resolved from the peak of nonscattered electrons. However, the energy resolution of the Trento apparatus is about 25 eV at this energy and therefore both peaks were merged in their transmission measurements. The magnitude of this error contribution can be estimated by taking into account that the relation between σ_T (in atomic units) and the transmission intensity (I), under the assumption of an ideal gas behaviour, is given by

$$I = I_0 \exp\left(\frac{-3.701T}{LP}\sigma_T\right), \tag{5}$$

where I_0 is the incident electron intensity, T is the absolute temperature in Kelvin, L is the length of the gas cell in centimetres and P is the gas pressure in milliTorr. The error in the total cross section due to the uncertainty in the measured transmitted intensity is then given by

$$\left|\frac{\Delta\sigma_T}{\sigma_T}\right| = \frac{3.701T}{LP\sigma_T}\left|\frac{\Delta I}{I}\right|. \tag{6}$$

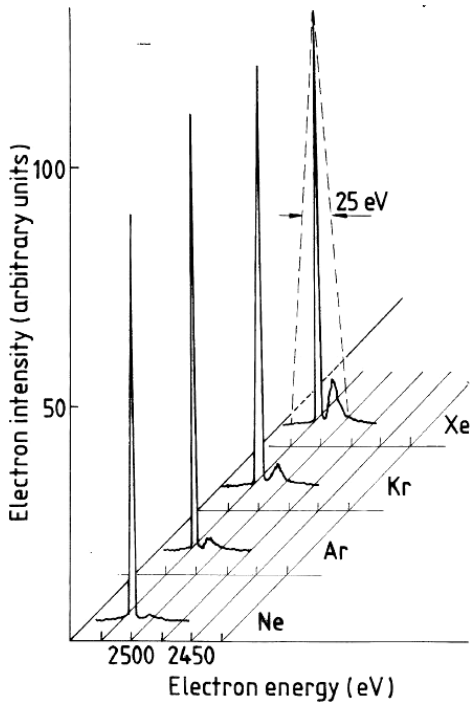

Figure 2. Energy spectra of transmitted electrons at 2525 eV incident energy and 10 mTorr of Ne, Ar, Kr and Xe, respectively, in the gas cell.

ΔI can be derived from figure 2 by measuring the area of the inelastic peak while I is given by the area of the 2525 eV electrons. Under these conditions we obtained that the error in the total cross section, due to a poor energy resolution, is of 4.2, 8.7, 10.9 and 18.2% for Ne, Ar, Kr and Xe, respectively. This result shows that the magnitude of the error contribution depends on the target. While in the case of Ne it is of the order of the other experimental errors, for Kr and Xe it is one order of magnitude larger. To calculate the total error driven by the electron scattered into the detection angle, the elastic contribution to the intensity of the transmitted electrons must be included. The magnitude of this contribution is strongly dependent on the scattering geometry and has been previously investigated for our experimental conditions [15] by means of a Monte Carlo simulation of the electron transport through the gas cell. The circular electron trajectories used in [4] made it difficult to carry out a similar study there. However, taking into account the conclusions of [15] and the angular resolution quoted in [4], a contribution of the elastic scattering to this effect of the same order as that for the inelastic one can be expected. By adding both the elastic and inelastic contributions, the above-mentioned discrepancy between our results and those of Zecca *et al* [4] can be explained, as well as its dependence on the size of the atomic targets. Concerning the evolution of this error at higher energies, the differential cross section at $\theta = 0$ tends to be a constant, independent of the incident energy, when the energy increases. As the total cross section decreases with energy, we can expect that this error contribution increases at least at the same rate as the total cross section decreases.

4.2. Elastic scattering cross sections

The differential and integral elastic cross sections calculated in this study are shown in table 2 for incident energies ranging from 50 to 10 000 eV. In order to compare with previous experimental

Table 2. Elastic cross sections for electron scattering by xenon in the energy range 50–10 000 eV. Differential cross sections are in a_0^2 sr^{-1} units and the integral values are in a_0^2 units.

Angle (deg)	Energy (eV)										
	50	100	200	400	500	750	1000	2000	3000	6000	10 000
0	85.6	123	160	203	218	243	263	314	348	406	443
1	79.5	111	144	181	193	212	226	258	275	293	293
2	69.4	95.4	123	152	160	172	179	189	189	174	150
3	61.4	82.5	106	128	133	140	142	137	128	101	77.1
4	54	71	91	108	111	112	110	97.7	85	58.5	40.1
5	47.6	61.1	77.9	90.1	91	89.3	85	68.2	55.5	34.1	22
6	42	52.5	66.8	75.2	74.7	70.4	64.9	47.4	36.4	21	13.3
7	37	45	57	62.3	60.8	55	49	32.8	24.3	13.6	8.63
8	32.7	38.4	48.6	51.4	49.2	42.7	36.8	23.1	16.8	9.35	5.83
9	28.9	32.7	41.2	42.1	39.6	33	27.6	16.6	12	6.65	4.09
10	25.5	27.7	34.7	34.4	31.7	25.4	20.8	12.3	8.89	4.85	2.97
11	22.5	23.3	29.1	27.9	25.3	19.6	15.8	9.32	6.76	3.64	2.24
12	19.9	19.4	24.3	22.6	20.2	15.3	12.3	7.28	5.25	2.8	1.7
13	17.5	16.1	20.1	18.3	16.1	12.1	9.67	5.78	4.14	2.18	1.3
14	15.4	13.1	16.5	14.8	13	9.67	7.79	4.68	3.32	1.75	1.06
15	13.5	10.6	13.6	12.1	10.6	7.88	6.39	3.82	2.69	1.41	0.877
16	11.8	8.43	11.1	9.99	8.72	6.54	5.33	3.17	2.22	1.18	0.754
17	10.3	6.59	9.06	8.35	7.31	5.52	4.5	2.64	1.84	0.989	0.607
18	8.99	5.06	7.46	7.08	6.22	4.71	3.84	2.24	1.56	0.85	0.497
19	7.79	3.81	6.22	6.1	5.37	4.07	3.3	1.9	1.33	0.73	0.42
20	6.73	2.83	5.28	5.34	4.69	3.54	2.86	1.63	1.14	0.632	0.373
21	5.79	2.07	4.6	4.73	4.14	3.1	2.49	1.42	1	0.552	0.331
22	4.95	1.52	4.11	4.23	3.68	2.72	2.18	1.23	0.88	0.482	0.276
23	4.22	1.16	3.79	3.82	3.29	2.4	1.92	1.09	0.786	0.428	0.233
24	3.58	0.943	3.58	3.47	2.95	2.13	1.7	0.968	0.701	0.376	0.2
25	3.01	0.859	3.46	3.17	2.66	1.9	1.51	0.87	0.632	0.335	0.184
26	2.52	0.88	3.39	2.9	2.4	1.69	1.35	0.784	0.569	0.296	0.165
27	2.1	0.983	3.37	2.66	2.17	1.52	1.21	0.712	0.517	0.265	0.144
28	1.74	1.15	3.37	2.44	1.96	1.36	1.09	0.649	0.47	0.237	0.125
29	1.43	1.36	3.37	2.23	1.77	1.23	0.99	0.594	0.428	0.213	0.112
30	1.16	1.59	3.37	2.04	1.6	1.11	0.904	0.546	0.391	0.192	0.103
35	0.365	2.69	3.09	1.24	0.95	0.723	0.615	0.368	0.256	0.121	0.064 5
40	0.093	3.04	2.29	0.721	0.607	0.53	0.455	0.258	0.177	0.081 9	0.044 2
45	0.0809	2.51	1.3	0.441	0.451	0.423	0.348	0.188	0.128	0.058 5	0.031 8
50	0.227	1.53	0.482	0.351	0.4	0.35	0.271	0.143	0.0977	0.043 5	0.023 9
55	0.477	0.61	0.0772	0.375	0.393	0.291	0.209	0.114	0.0773	0.033 6	0.018 6
60	0.753	0.0824	0.111	0.442	0.387	0.234	0.162	0.094	0.0629	0.026 8	0.015
65	0.946	0.0336	0.45	0.484	0.354	0.177	0.125	0.0801	0.052	0.021 7	0.012 1
70	0.955	0.334	0.881	0.462	0.288	0.127	0.1	0.0698	0.0435	0.018 1	0.009 8
75	0.758	0.75	1.2	0.372	0.197	0.089 1	0.088	0.0616	0.0369	0.015 4	0.008 06
80	0.426	1.06	1.28	0.237	0.105	0.071 3	0.086 7	0.0544	0.0313	0.013 4	0.006 75
85	0.115	1.15	1.11	0.103	0.0413	0.075 4	0.093 7	0.0476	0.0267	0.011 9	0.005 73
90	0.0091	1	0.768	0.0171	0.0274	0.099 4	0.104	0.0412	0.0232	0.010 8	0.004 94
95	0.243	0.725	0.393	0.0136	0.0716	0.134	0.112	0.035	0.0207	0.010 2	0.004 38
100	0.841	0.45	0.119	0.0993	0.163	0.167	0.113	0.0293	0.019	0.009 72	0.003 95
110	2.57	0.261	0.132	0.421	0.367	0.181	0.082 4	0.0217	0.0186	0.009 3	0.003 35
120	3.41	0.45	0.606	0.606	0.39	0.101	0.028	0.0237	0.0224	0.009 46	0.003 19
130	2.26	0.39	0.763	0.417	0.186	0.007 52	0.009 41	0.0405	0.03	0.009 88	0.003 15
150	0.587	0.268	0.0359	0.149	0.257	0.34	0.298	0.115	0.0521	0.011 1	0.003 53
180	10.6	4.57	1.69	2.08	2.05	1.42	0.899	0.205	0.0747	0.011 9	0.014 5
Integral	24.36	18.24	20.25	16.9	15.39	12.79	11.12	7.847	6.322	4.264	3.129

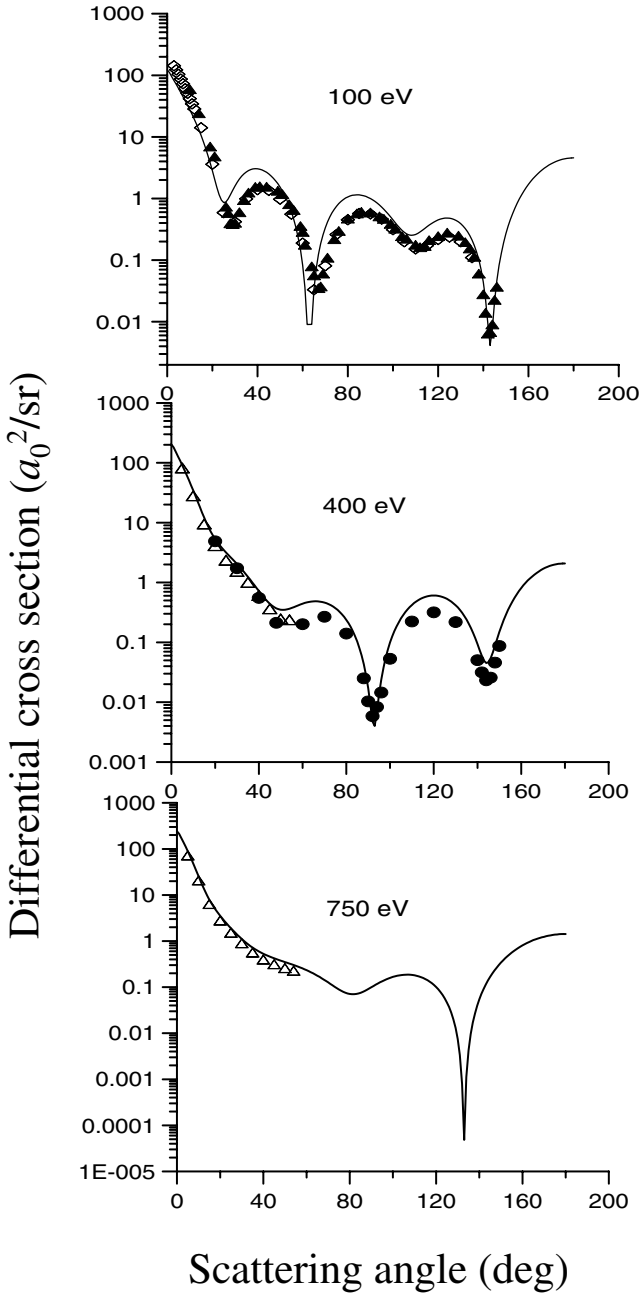

Figure 3. Differential elastic cross sections of Xe for 100, 400 and 750 eV incident electron energies. —— present calculations; ▲, Register *et al* [17]; ◇, Ester and Kessler [18]; ●, Williams and Crowe [19]; △, Jansen and de Heer [20].

results, differential elastic cross sections for some incident energies are shown in figure 3 (100, 400 and 750 eV) and in figure 4 (1000, 3000 and 8000 eV). As these figures show, there is a general agreement between our calculations and the results of Register *et al* [17], Ester and

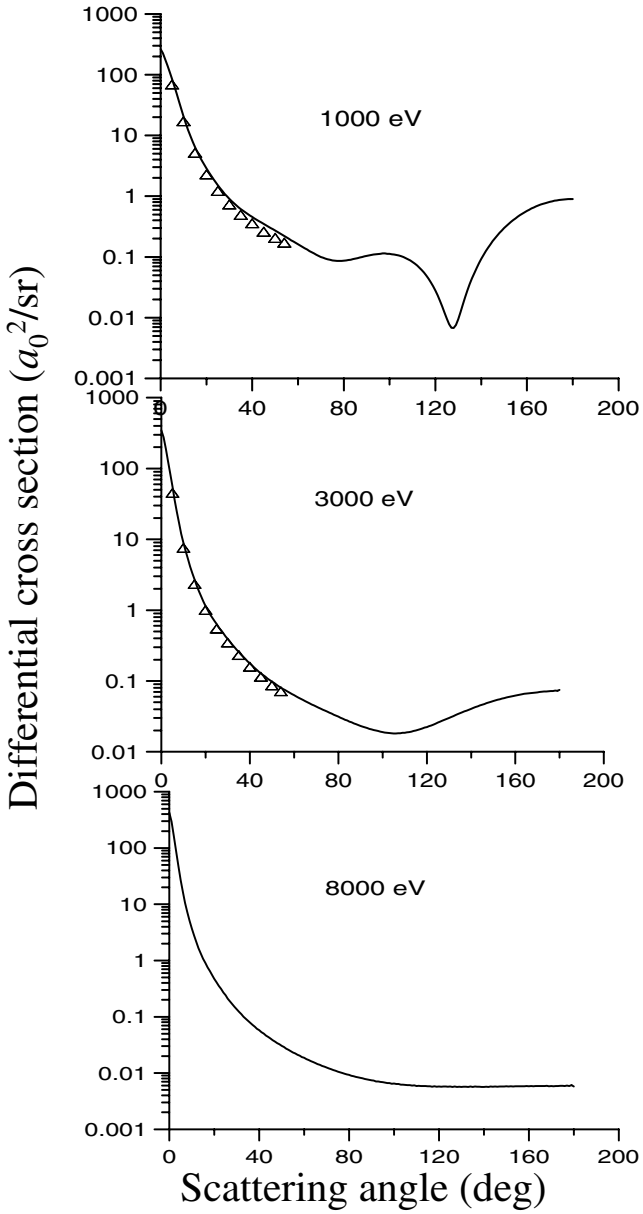

Figure 4. Differential elastic cross sections of Xe for 1000, 3000 and 8000 eV incident electron energies. —— this work; △, Jansen and de Heer [20].

Kessler [18], Williams and Crowe [19] and Jansen and de Heer [20] for incident energies of 100, 400, 750, 1000 and 3000 eV, respectively. However, the agreement tends to be less satisfactory at low energies, where only a few partial waves take part in the process, and therefore the calculated cross sections are more sensitive to the accuracy of the Hartree–Fock procedure used to describe the target.

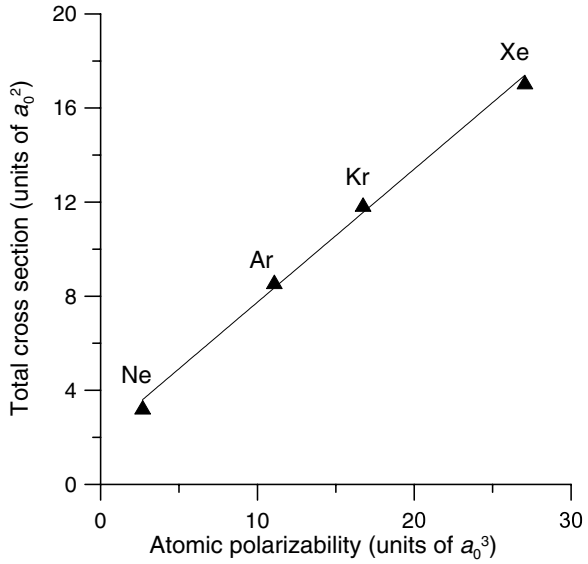

Figure 5. Total electron scattering cross sections for Ne, Ar, Kr and Xe for 1000 eV incident energy as a function of the atomic polarizability of the target.

4.3. Empirical formulae

Empirical formulae reproducing experimental data are very useful in computational applications and show interesting regularities which allow one to extrapolate cross section data to other atomic targets [21]. As shown in [21], for energies above 500 eV there is a correlation between the total electron scattering cross section (σ_T) on Ne, Ar and Kr and other atomic parameters, such as the polarizability (α) and the number of target electrons (Z), that can be represented by

$$\sigma_T = A(\alpha)E^{-B(Z)}, \tag{7}$$

where parameters $A(\alpha)$ and $B(Z)$ were fitted to the experimental results. The fitting procedure of [21] can be repeated including in this case our results on Xe. For a given energy, $A(\alpha)$ represents the dependence on the total cross section with the atomic polarizability. As figure 5 shows, for Ne, Ar, Kr and Xe at an incident energy of 1000 eV it can be fitted to a straight line and gives directly the $A(\alpha)$ value:

$$A(\alpha) = 0.57\alpha + 2.08. \tag{8}$$

$B(Z)$ is then derived from the energy dependence of the total cross section for each atom which figure 6 shows on a logarithmic scale. According to figure 7, this parameter can be fitted to

$$B(Z) = 0.89 - 0.0063Z. \tag{9}$$

Empirical values obtained by introducing (6) and (7) in (5) are plotted in figure 8 for incident energies ranging from 500 to 10 000 eV. As can be seen in this figure, for the energy range 500–5000 eV, equation (5) reproduces the experimental data for Ne, Ar, Kr and Xe to within 10% and can be used to extrapolate total cross section values to higher energies.

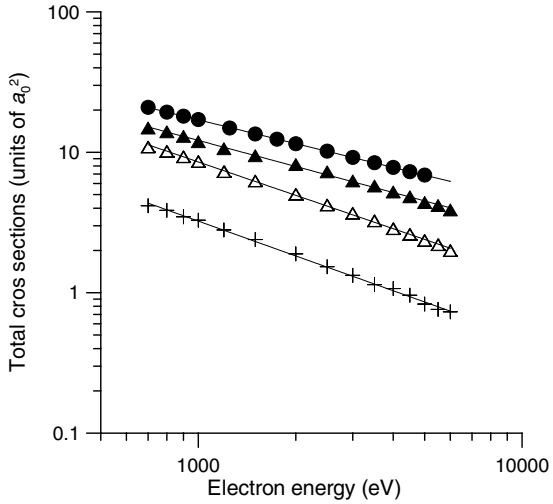

Figure 6. Energy dependence of the total electron scattering cross section from (+) Ne, (△) Ar, (▲) Kr and (●) Xe in the energy range 500–5000 eV.

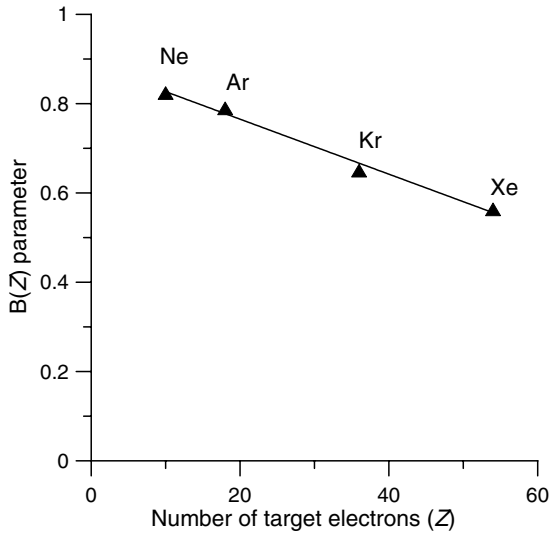

Figure 7. $B(Z)$ parameter of equation (5) for Ne, Ar, Kr and Xe as a function of the number of target electrons.

5. Conclusions

Experimental total electron scattering cross sections from Xe in the energy range 300–5000 eV have been obtained with a total error of about 3%. Using a scattering potential method, which includes relativistic effects, differential and integral elastic cross sections have been also calculated for electron energies ranging from 50 to 10 000 eV. The discrepancy in the high-energy total electron scattering cross section data between our previous measurements and those of the group of Trento have been plausibly justified. Finally, an empirical formula based on the strong dependence observed for the electron scattering total cross sections of

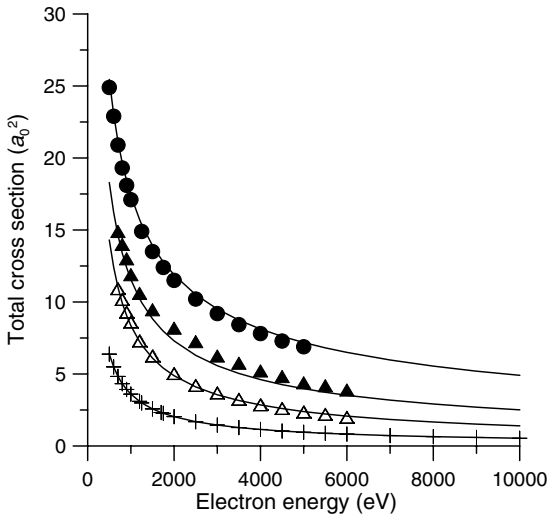

Figure 8. (——) empirical total cross section data given by equations (5), (6) and (9) for energies from 500 to 10 000 eV compared with the experimental values for (+) Ne, (△) Ar, (▲) Kr and (●) Xe.

noble gases on the atomic poralizability and the number of target electrons is given. This expression reproduces our measured high-energy total cross sections for Ne, Ar, Kr and Xe to within 10% and may be useful for extrapolating data at higher energies.

Acknowledgments

This work has been partially supported by the Programa Nacional de Promoción General del Conocimiento (project BFM2000-0012).

References

[1] Trajmar S, Register D F and Chutjian A 1983 *Phys. Rep.* **97** 219
[2] Zecca A, Karwasz G P and Brusa R 1996 *Riv. Nuovo Cimento* **19** 43
[3] García G, Arqueros F and Campos J 1986 *J. Phys. B: At. Mol. Phys.* **19** 3777
[4] Zecca A, Karwasz G, Brusa R S and Grisenti R 1991 *J. Phys. B: At. Mol. Opt. Phys.* **24** 2737
[5] Brusa R S, Karwasz G P and Zecca A 1996 *Z. Phys.* D **38** 379
[6] García G, Roteta M, Manero F, Blanco F and Williart A 1999 *J. Phys. B: At. Mol. Opt. Phys.* **32** 1783
[7] Zecca A, Karwasz G P and Brusa R S 2000 *J. Phys. B: At. Mol. Opt. Phys.* **33** 843
[8] Willian H P 1994 *Numerical Recipes on Fortran* (Cambridge: Cambridge University Press)
[9] Calogero F 1967 *Variable Phase Approach to Potential Scattering* (New York: Academic)
[10] Wagenaar R W and de Heer F J 1985 *J. Phys. B: At. Mol. Phys.* **18** 2021
[11] Dababneh M S, Hsieh Y-F, Kauppila W E, Pol V and Stein T S 1982 *Phys. Rev.* A **26** 1252
[12] Nickel J H, Imre K, Register D F and Trajmar S 1985 *J. Phys. B: At. Mol. Phys.* **18** 125
[13] Szmytkowski Cz, Maciag K and Karwasz G 1996 *Phys. Scr.* **54** 271
[14] Karwasz G, Brusa R S, Gasparoli A and Zecca A 1993 *Chem. Phys. Lett.* **211** 529
[15] García G, Roteta M and Manero F 1997 *Chem. Phys. Lett.* **264** 589
[16] García G and Blanco F 2001 *Phys. Lett.* A **279** 61
[17] Register D F, Vuscovic L and Trajmar S 1986 *J. Phys. B: At. Mol. Phys.* **19** 1685
[18] Ester T and Kessler J 1994 *J. Phys. B: At. Mol. Opt. Phys.* **27** 4295
[19] Williams J F and Crowe A 1975 *J. Phys. B: At. Mol. Phys.* **8** 2233
[20] Jansen R H J and de Heer F J 1976 *J. Phys. B: At. Mol. Phys.* **9** 213
[21] Williart A and García G 2001 *Phys. Scr.* **64** 343